

Effect of orbital symmetry on atomic ionization in near-infrared laser fields

Manqi Xu(徐嫚琦), Shilin Hu(胡师林), Li Guo(郭丽), and Jing Chen(陈京)

Citation: Chin. Phys. B, 2025, 34 (**1**): 013202. DOI: 10.1088/1674-1056/ad8dbe
Journal homepage: http://cpb.iphy.ac.cn; http://iopscience.iop.org/cpb

What follows is a list of articles you may be interested in

Wavelength- and ellipticity-dependent photoelectron spectra from multiphoton ionization of atoms

Keyu Guo(郭珂雨), Min Li(黎敏), Jintai Liang(梁锦台), Chuanpeng Cao(曹传鹏), Yueming Zhou(周月明), and Peixiang Lu((陆培祥)
Chin. Phys. B, 2023, 32 (**2**): 023201. DOI: 10.1088/1674-1056/ac9b36

Accurate electron affinity of atomic cerium and excited states of its anion

Xiao-Xi Fu(付筱茜), Ru-Lin Tang(唐如麟), Yu-Zhu Lu(陆禹竹), Chuan-Gang Ning(宁传刚)
Chin. Phys. B, 2020, 29 (**7**): 073201. DOI: 10.1088/1674-1056/ab90e9

Interpulse interference of electron emission from an atom irradiated by sinusoidally phase-modulated pulse

Hai-Ying Yuan(袁海颖), Fu-Ming Guo(郭福明), Di-Yu Zhang(张頔玉), Jun Wang(王俊), Ji-Gen Chen(陈基根), Yu-Jun Yang(杨玉军)
Chin. Phys. B, 2018, 27 (**10**): 103201. DOI: 10.1088/1674-1056/27/10/103201

Simultaneous study of the lower order harmonic and photoelectron emission from an atom in intense laser pulse

Yan Yan(闫妍), Fu-Ming Guo(郭福明), Jun Wang(王俊), Ji-Gen Chen(陈基根), Yu-Jun Yang(杨玉军)
Chin. Phys. B, 2018, 27 (**8**): 083202. DOI: 10.1088/1674-1056/27/8/083202

Photoelectron angular distributions of H ionization in low energy regime: Comparison between different potentials

Shu-Na Song(宋舒娜), Hao Liang(梁昊), Liang-You Peng(彭良友), Hong-Bing Jiang(蒋红兵)
Chin. Phys. B, 2016, 25 (**9**): 093201. DOI: 10.1088/1674-1056/25/9/093201

Effect of orbital symmetry on atomic ionization in near-infrared laser fields

Manqi Xu(徐嫚琦)[1], Shilin Hu(胡师林)[1,2,†], Li Guo(郭丽)[3], and Jing Chen(陈京)[4,5]

[1] *Research Center for Advanced Optics and Photoelectronics, Department of Physics, College of Science, Shantou University, Shantou* 515063, *China*
[2] *Key Laboratory of Intelligent Manufacturing Technology of MOE, Shantou University, Shantou* 515063, *China*
[3] *Department of Physics, Shanghai Normal University, Shanghai* 200234, *China*
[4] *Hefei National Research Center for Physical Sciences at the Microscale and School of Physical Sciences, Department of Modern Physics, University of Science and Technology of China, Hefei* 230026, *China*
[5] *Shenzhen Key Laboratory of Ultraintense Laser and Advanced Material Technology, Center for Advanced Material Diagnostic Technology, and College of Engineering Physics, Shenzhen Technology University, Shenzhen* 518118, *China*

(Received 23 August 2024; revised manuscript received 18 October 2024; accepted manuscript online 1 November 2024)

We have performed a comparative study of the photoelectron spectra adopting different initial states (2s or $2p_0$) of hydrogen atoms in a near-infrared laser pulse by using the full three-dimensional time-dependent Schrödinger equation. It is demonstrated that the atomic photoelectron spectra oscillate out of step as a function of electron kinetic energies for different initial states (2s or $2p_0$), which is well reproduced by the simulations based on strong field approximation, and the above distinct feature is ascribed to the different interferences from the partial electron wave packets detached by positive and negative electric fields for different initial states of 2s and $2p_0$.

Keywords: orbital symmetry, photoelectron spectra, strong-field approximation

PACS: 32.30.–r, 32.80.Fb, 31.15.A–

DOI: 10.1088/1674-1056/ad8dbe **CSTR:** 32038.14.CPB.ad8dbe

1. Introduction

Ionization of atoms exposed to intense laser pulses is a fundamental process in a multitude of research fields, especially in the emerging area of attosecond science, because atomic ionization is an initial key process in a wealth of intriguing strong-field physical phenomena, such as above-threshold ionization (ATI),[1,2] high-order harmonic generation (HHG),[3–6] and nonsequential double ionization (NSDI).[7–9] In addition, the ionization dynamics of atoms subjected to strong laser fields has attracted widespread experimental and theoretical studies in the past three decades.

The impacts of the initial electron cloud distribution on atomic ionization have gained considerable attention in recent years. It is shown that photoelectron momentum distributions (PMDs) carry a clear signature of the imprint of the orbital angular node when Ar atoms are exposed to an intense elliptically polarized laser pulse.[10,11] It is demonstrated that the tunneling ionization is more likely to occur for a counter-rotating electron with respect to a corotating electron when atoms are subjected to circularly polarized laser pulses,[12–14] which indicates that the ionization dynamics are sensitive to the initial magnetic quantum number m. This intriguing ionization behavior has been experimentally observed in the double ionization of Ar atoms in near-circularly polarized laser fields.[15] More recently, theoretical calculations indicate that tunneling ionization and tunneling exits sensitively depend on the initial atomic orbital structures for atoms in elliptically polarized laser fields.[16,17] In addition, it has been found that the asymptotic behavior of an initial wave function has an important impact on the main shape of PMDs possessing large momenta for F^- ions in an orthogonal two-color laser field.[18]

Photoelectron spectra of atoms subjected to strong laser fields have recently attracted experimental and theoretical investigations. For the electron kinetic energy less than $2U_p$ (U_p is the ponderomotive energy), the photoelectron spectrum decreases exponentially, which originates from the contributions of the direct ionization. Surprising experimental discoveries in this area continue to show up. For instance, a prominent low-energy structure is observed in the low-energy part of the energy spectra, which is unanimously ascribed to the effect of the Coulomb potential of the parent ion.[19] This intriguing physical phenomenon has recently drawn attention in the strong-field physics community.[20–23] The high-energy spectrum comprises a flat plateau extending to $10U_p$, which stems from the elastic scattering of the electron when it recollides with the core in the backward direction. For the high-energy part of the energy spectra, one intriguing feature is the appearance of the resonance-like enhancement (RLE) of groups of adjacent peaks in the plateau regime,[24,25] which is sensitive to the laser's parameters. The aforementioned distinct characteristic is ascribed to multiphoton resonance with laser-dressed excited bound states obtained by *ab initio* calculations

†Corresponding author. E-mail: shlhu@stu.edu.cn

© 2025 Chinese Physical Society and IOP Publishing Ltd. All rights, including for text and data mining, AI training, and similar technologies, are reserved.

or channel closing effect within the framework of strong field approximation.[26–31] Recent experimental observations indicate that the RLE structure shows strong dependence on the initial molecular orbital.[32–34]

As stated earlier, the initial electron cloud distribution plays a vital role in atomic ionization in intense laser fields and the characteristics of molecular photoelectron spectra depend on the initial molecular orbital.[32–35] However, a complete description of the role of atomic orbital in photoelectron spectra, given in a detailed manner based on a quantitative analysis, is still missing. In this work, we have carried out a comparison study of the photoelectron spectra using different initial states (2s or $2p_0$) for H atoms subjected to a near-infrared laser field by means of *ab initio* approaches and strong field approximation. We have found that the atomic photoelectron spectra oscillate in an inverse manner with increasing electron kinetic energies for different initial states (2s or $2p_0$), which has been ascribed to the different interferences between the subwaves of the released electron by the negative and the positive electric fields due to the different parities of initial states. Atomic units (a.u.) are used unless otherwise indicated.

2. Theoretical methods

2.1. Time-dependent Schrödinger equation

Within dipole approximation and the velocity gauge, the time-dependent Schrödinger equation (TDSE) of hydrogen atom subjected to the laser pulse is given by

$$\mathrm{i}\frac{\partial}{\partial t}\Psi(\boldsymbol{r},t)=[H_0(\boldsymbol{r})-\mathrm{i}\boldsymbol{A}(t)\cdot\nabla]\Psi(\boldsymbol{r},t). \tag{1}$$

The details of single-electron Hamiltonian $H_0(\boldsymbol{r}) = -(1/2)\nabla^2 - 1/r$ can be found in Ref. [36]. The vector potential is written as $\boldsymbol{A}(t) = E_0/\omega \sin^2(\pi t/t_{\max})\cos(\omega t)\hat{z}$ $(0 < t < t_{\max})$ with unit vector $\hat{z}$. E_0 indicates the peak electric strength, and $t_{\max}$ and ω denote the duration and the angular frequency of the laser pulse, respectively. The laser–atom interaction is treated in the velocity gauge because the calculations in the velocity gauge converge much faster with respect to those in the length gauge.[37,38] The time-varying wave function is expanded in terms of B-splines in the following form:

$$\Psi(r,\xi,\varphi,t)=\frac{1}{\sqrt{2\pi}}\sum_{\mu\nu}C_{\mu\nu}(t)\frac{B_\mu^k(r)}{r}B_\nu^k(\xi)(1-\xi^2)^{\frac{|m|}{2}}\,\mathrm{e}^{\mathrm{i}m\varphi}, \tag{2}$$

where $\xi = \cos\theta$, and $k = 9$ indicates the order of B-splines.[36,39] The above time-dependent wave function is evolved by the Crank–Nicolson approach.[36,39,40]

The photoelectron spectra can be obtained by employing the window-operator approach,[41] which is highly efficient to extract the photoelectron spectra from the wave function after the laser pulse is switched off. A window operator is adopted to calculate the probability of finding an electron in a final-state "energy bin" of a width of 2γ centered around E_k

$$\hat{W}(E_k,\nu,\gamma)=\frac{\gamma^{2^\nu}}{(H_0-E_k)^{2^\nu}+\gamma^{2^\nu}}, \tag{3}$$

where $\nu = 2$ and $\gamma = 0.005$ a.u. are employed in the following simulations and the energy levels E_k are obtained by a diagonalization procedure of the field-free Hamiltonian matrix.

In the following calculations, the truncated radius is $r_{\max} = 900$ a.u., and 1400 B-splines and 40 B-splines are adopted in the radial direction and the angular direction, respectively. The initial state is 2s or $2p_0$ of field-free H atom. The magnetic quantum number $m = 0$ is a good quantum number because a linearly polarized laser pulse is used in our simulations. The atom is exposed to a two-cycle laser pulse of frequency $\omega = 0.0285$ a.u. ($\lambda = 1600$ nm) and intensity 20 TW/cm^2, and the time step is $\Delta t = 0.02$ a.u. Convergence of the numerical simulations is achieved with the above settings.

2.2. Strong field approximation

In the present work, the atomic ionization is also examined by strong-field approximation (SFA).[42–44] The vector potential is $\boldsymbol{A}(t) = E_0\cos(\omega t)\hat{z}/\omega$ with unit vector $\hat{z}$, and the single ionization rate obtained by SFA in the length gauge is given by[40,45,46]

$$W=2\pi N_\mathrm{e}\sum_{n=n_0}^{\infty}\int|T_{pn}|^2\delta(E_p+I_\mathrm{p}-n\omega)\,\mathrm{d}\boldsymbol{p}, \tag{4}$$

$$T_{pn}=\frac{1}{T}\int_0^\mathrm{T}\mathrm{d}t'\exp\left[\mathrm{i}S(t',\boldsymbol{p})\right]E_0\sin\omega t'\widetilde{\phi}(\boldsymbol{M}_p) \tag{5}$$

with the action

$$S(t',\boldsymbol{p})=\frac{E_0^2}{8\omega^3}\sin 2\omega t'+\frac{E_0\hat{z}\cdot\boldsymbol{p}}{\omega^2}\sin\omega t'+(\frac{p^2}{2}+I_\mathrm{p}+U_\mathrm{p})t'. \tag{6}$$

Here N_e indicates the number of equivalent electrons in the valence orbital and n_0 is the minimum number of photons required to ionize the atom. $E_p = p^2/2 + U_\mathrm{p}$ represents the quasienergy with the kinetic energy of the emitted electron by absorption of n photons $p^2/2 = n\omega - U_\mathrm{p} - I_\mathrm{p}$ and the ponderomotive energy $U_\mathrm{p} = E_0^2/(4\omega^2)$. $\widetilde{\phi}(\boldsymbol{M}_p)$ represents the dipole matrix element,[46] and $\boldsymbol{M}_p = \boldsymbol{p} + \boldsymbol{A}(t')$ and t' indicate the mechanical momentum and the ionization moment, respectively. The peak electric field amplitude of the intense laser pulse E_0 corresponds to the intensity of 20 TW/cm^2, and the angular frequency is $\omega = 0.0285$ a.u. The initial states of 2s and $2p_0$ are written as $\varphi_{2s}(\boldsymbol{r}) = 1/\sqrt{8\pi}(1-r/2)\,\mathrm{e}^{-r/2}$ and $\varphi_{2p_0}(\boldsymbol{r}) = 1/\sqrt{32\pi}r\,\mathrm{e}^{-r/2}\cos\theta$, respectively, and the ionization energy of the target is $I_\mathrm{p} = 0.125$ a.u. In the present work, Eqs. (4) and (5) are obtained by numerical integration.

3. Results and discussion

In Fig. 1, we depict the photoelectron spectra calculated by TDSE and SFA simulations for the initial states of 2s and $2p_0$. It is demonstrated that the photoelectron spectra show oscillation structures as a function of kinetic energies of the detached electron for different initial states, while the above oscillatory behaviors are out of phase for initial states of 2s and $2p_0$ for TDSE calculations in Fig. 1(a), which are qualitatively reproduced by SFA simulations in Fig. 1(b). The positions of the humps and dips in Figs. 1(a) and 1(b) are not exactly the same. This happens because the role of the Coulomb potential in continuum states is not considered in the SFA simulations with respect to TDSE calculations.

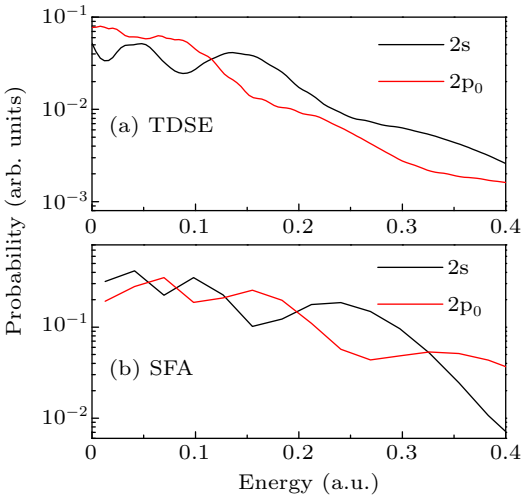


Fig. 1. Photoelectron spectra obtained by TDSE (a) and SFA (b) for the initial states of 2s and $2p_0$.

Because the SFA calculations are qualitatively consistent with the TDSE simulations, we can uncover the physical mechanisms of the above distinct phenomena from SFA simulations in the following analysis. We choose the photoelectron spectra of the electron emitted along the polarization direction of the laser field for illustration in Fig. 2(a). It is also shown that the photoelectron spectra oscillate in an inverse manner with the increase of the kinetic energies of the emitted electron for initial states of 2s and $2p_0$, which is in good accordance with the results in Fig. 1(b). According to Eqs. (4) and (5), the photoelectron spectra contain the contributions of the electronic wave packets detached by the positive and the negative electric fields. In order to shed more physical insights into the results in Fig. 2(a), we calculate the contribution to the ionization for the electron released by the positive electric field and the negative electric field, and show the phase differences of the ionization amplitudes obtained in the two ionization time domains in Fig. 2(b).

In Fig. 2(b), it is demonstrated that the phase differences oscillate as a function of the kinetic energies of the emitted electron and the phase differences show out-of-phase oscillation structures with increasing kinetic energies of the released electron for the initial state 2s compared with that of $2p_0$ state. For the initial state 2s, the phase difference approaches π around the kinetic energy 0.15 a.u., while the phase differences are close to 0 near the kinetic energies of 0.1 a.u. and 0.25 a.u. Therefore, the ionization amplitudes from the electronic wave packets detached by the negative and positive electric fields tend to cancel each other due to destructive interference around the kinetic energy 0.15 a.u., giving rise to a considerably lower yield. In contrast, the ionization amplitudes from the electron released by the negative and positive electric fields prefer to interfere constructively, resulting in a relatively higher yield near the kinetic energies of 0.1 a.u. and 0.25 a.u. For the initial state $2p_0$, the phase differences approach π around the kinetic energies of 0.1 a.u. and 0.2 a.u., while the phase difference is close to 0 about the kinetic energy 0.15 a.u. The constructive interference occurs for the electronic wave packet with kinetic energy 0.15 a.u., and destructive interference takes place near the kinetic energies of 0.1 a.u. and 0.2 a.u., which give rise to the structures of humps and dips in the photoelectron spectra around the above corresponding kinetic energies. Consequently, the humps and dips in the photoelectron spectra stem from the constructive and destructive interferences between the partial electronic wave packets released by the negative and the positive electric fields, respectively. In Fig. 3, the PMDs of hydrogen atoms (2s and 2p) are also calculated by SFA calculations. It is found that the stripes show up out of phase for different initial states in Fig. 3, which are in good accordance with the photoelectron spectra of hydrogen atoms (2s and 2p) in Fig. 1(b).

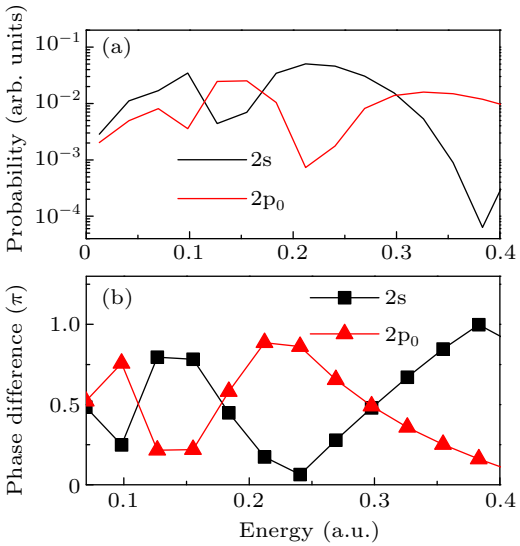


Fig. 2. (a) Photoelectron spectra of the electron calculated by SFA with canonical momenta $\boldsymbol{p}$ parallel to the direction of the electric fields adopting different initial states (2s and $2p_0$). (b) Phase differences of the ionization amplitudes in Eq. (4) for an electron detached in the positive and negative electric fields with canonical momenta $\boldsymbol{p}$ parallel to the polarization direction of the laser pulse employing initial states of 2s and $2p_0$.

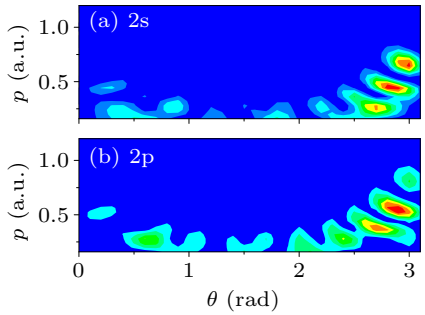


Fig. 3. Photoelectron momentum distributions obtained by SFA simulations for hydrogen atoms (2s and 2p) in the laser field.

The parities of initial states 2s and $2p_0$ are even and odd, respectively, so an additional phase of π is introduced for the action of the initial state $2p_0$ compared with that of 2s state

$$S_{2p_0}(t', \boldsymbol{p}) = S_{2s}(t', \boldsymbol{p}) + \pi, \tag{7}$$

which gives rise to the different interferences between the subwaves of the emitted electron by the negative and the positive electric fields for different initial states in Fig. 2(b).

4. Conclusions

In summary, we have performed a comparison study of the ionization dynamics of H atoms possessing different initial states (2s and $2p_0$) subjected to a short near-infrared laser pulse adopting TDSE and SFA calculations. It is found that photoelectron spectra exhibit out-of-phase oscillatory structures with the increase of electron kinetic energies for different initial states of 2s and $2p_0$ based on TDSE and SFA simulations. This intriguing feature stems from different interference effects from the electronic wave packets emitted by the negative and positive electric fields due to the different orbital symmetries of 2s and $2p_0$ states.

Acknowledgments

Project supported by Li Ka Shing Foundation STU-GTIIT Joint Research (Grant No. 2024LKSFG02), the STU Scientific Research Foundation for Talents (Grant Nos. NTF22026, NTF23011, NTF23014, and NTF23036T), the National Basic Research Program of China (Grant No. 2019YFA0307700), and the National Natural Science Foundation of China (Grant Nos. 12074239 and 12274300).

References

[1] Agostini P, Fabre F, Mainfray G, Petite G and Rahman N 1979 *Phys. Rev. Lett.* **42** 1127
[2] Becker W, Grasbon F, Kopold R, Milošević D, Paulus G and Walther H 2002 *Adv. At. Mol. Opt. Phys.* **48** 35
[3] L'Huillier A and Balcou Ph 1993 *Phys. Rev. Lett.* **70** 774
[4] Corkum P B 1993 *Phys. Rev. Lett.* **71** 1994
[5] Schafer K, Yang B, Dimauro L and Kulander K 1993 *Phys. Rev. Lett.* **70** 1599
[6] Krausz F and Ivanov M 2009 *Rev. Mod. Phys.* **81** 163
[7] Fittinghoff D, Bolton P, Chang B and Kulander K 1992 *Phys. Rev. Lett.* **69** 2642
[8] Walker B, Sheehy B, DiMauro L, Agostini P, Schafer K and Kulander K 1994 *Phys. Rev. Lett.* **73** 1227
[9] Becker W, Liu X J, Ho P and Eberly J 2012 *Rev. Mod. Phys.* **84** 1011
[10] Martiny C, Abu-samha M and Madsen L 2010 *Phys. Rev. A* **81** 063418
[11] Abu-samha M and Madsen L B 2011 *Phys. Rev. A* **84** 023411
[12] Barth I and Smirnova O 2011 *Phys. Rev. A* **84** 063415
[13] Barth I and Smirnova O 2013 *Phys. Rev. A* **87** 013433
[14] Walker S, Kolanz L, Venzke J and Becker A 2021 *Phys. Rev. A* **103** L061101
[15] Herath T, Yan L, Lee S K and Li W 2012 *Phys. Rev. Lett.* **109** 043004
[16] Zhang Q B, Basnayake G, Winney A, Lin Y, Debrah D, Lee S and Li W 2017 *Phys. Rev. A* **96** 023422
[17] Wang J P and He F 2017 *Phys. Rev. A* **95** 043420
[18] Chen J H, Han M, Xiao X, Peng L Y and Liu Y Q 2018 *Phys. Rev. A* **98** 033403
[19] Quan W, Lin Z, Wu M, Kang H, Liu H, Liu X, Chen J, Liu J, He X, Chen S, Xiong H, Guo L, Xu H, Fu Y, Cheng Y and Xu Z Z 2009 *Phys. Rev. Lett.* **103** 093001
[20] Blaga C I, Catoire F, Colosimo P, Paulus G, Muller H, Agostini P and DiMauro L 2009 *Nat. Phys.* **5** 335
[21] Liu C and Hatsagortsyan K 2010 *Phys. Rev. Lett.* **105** 113003
[22] Wu C Y, Yang Y D, Liu Y Q, Gong Q H, Wu M Y, Liu X, Hao X L, Li W D, He X T and Chen J 2012 *Phys. Rev. Lett.* **109** 043001
[23] Guo L, Han S S, Liu X, Cheng Y, Xu Z Z, Fan J, Chen J, Chen S, Becker W, Blaga C, DiChiara A, Sistrunk E, Agostini P and DiMauro L 2013 *Phys. Rev. Lett.* **110** 013001
[24] Hansch P, Walker M and Van Woerkom L 1997 *Phys. Rev. A* **55** 2535
[25] Hertlein M, Bucksbaum P and Muller H 1997 *J. Phys. B* **30** L197
[26] Muller H and Kooiman F 1998 *Phys. Rev. Lett.* **81** 1207
[27] Muller H 1999 *Phys. Rev. A* **60** 1341
[28] Potvliege R and Vučić S 2006 *Phys. Rev. A* **74** 023412
[29] Li B, Hu S, Shu Z, He X and Chen J 2018 *Opt. Express* **26** 13012
[30] Kopold R and Becker W 1999 *J. Phys. B* **32** L419
[31] Paulus G, Grasbon F, Walther H, Kopold R and Becker W 2001 *Phys. Rev. A* **64** 021401
[32] Cornaggia C 2010 *Phys. Rev. A* **82** 053410
[33] Quan W, Lai X Y, Chen Y J, Wang C L, Hu Z L, Liu X J, Hao X L, Chen J, Hasović E, Busuladžić M, Becker W and Milošević D B 2013 *Phys. Rev. A* **88** 021401
[34] Wang C, Okunishi M, Hao X, Ito Y, Chen J, Yang Y, Lucchese R, Zhang M, Yan B, Li W D, Ding D and Ueda K 2016 *Phys. Rev. A* **93** 043422
[35] Sun T, Zhang S W, Wang R, Feng S, Liu Y, Lv H and Xu H F 2020 *Chin. Phys. Lett.* **37** 043301
[36] Hu S L, Zhao Z X and Shi T Y 2014 *Int. J. Quan. Chem.* **114** 441
[37] Cormier E and Lambropoulos P 1996 *J. Phys. B: At. Mol. Opt. Phys.* **29** 1667
[38] Han Y C and Madsen L B 2010 *Phys. Rev. A* **81** 063430
[39] Bachau H, Cormier E, Decleva P, Hansen J E and Martín F 2001 *Rep. Pro. Phys.* **64** 1815
[40] Hu S, Shu Z, Liu M, Guo L, Hao X, Chen J and Lee C 2018 *Opt. Express* **26** 32225
[41] Schafer K J and Kulander K C 1990 *Phys. Rev. A* **42** 5794
[42] Keldysh L V 1964 *Zh. Eksp. Teor. Fiz.* **47** 1945
[43] Faisal F 1973 *J. Phys. B* **6** L89
[44] Reiss H 1980 *Phys. Rev. A* **22** 1786
[45] Milošević D 2006 *Phys. Rev. A* **74** 063404
[46] Li Y, Jia X Y, Yang S P, Li W D and Chen J 2010 *Chin. Phys. B* **19** 063302